

# Direct laser trapping for measuring the behavior of transfused erythrocytes in a sickle cell anemia patient

Aline Pellizzaro,<sup>2</sup> Gabriel Welker,<sup>1</sup> David Scott,<sup>2</sup> Rance Solomon,<sup>1</sup> James Cooper,<sup>1</sup> Anthony Farone,<sup>2</sup> Mary Farone,<sup>2</sup> Robert S. Mushi,<sup>3</sup> Maria del Pilar Aguinaga,<sup>3,4</sup> and Daniel Erenso<sup>\*,1</sup>

<sup>1</sup>Department of Physics & Astronomy, Middle Tennessee State University, Murfreesboro, Tennessee, 37132, USA

<sup>2</sup>Department of Biology, Middle Tennessee State University, Murfreesboro, Tennessee, 37132, USA

<sup>3</sup>Department of Obstetrics and Gynecology, Meharry Medical College Nashville, Tennessee 37208, USA

<sup>4</sup>Meharry Sickle Cell Center, Meharry Medical College Nashville, Tennessee 37208, USA

\*derenso@mtsu.edu

**Abstract:** Using a laser trap, we have studied the properties of erythrocytes from a sickle cell anemia patient (SCA) after receiving an intravenous blood transfusion, and a normal adult individual carrying normal adult hemoglobin. The hemoglobin type and quantitation assessment was carried out by high performance liquid chromatography (HPLC). We conducted an analysis of the size distributions of the cells. By targeting those erythrocytes in the overlapping regions of size distributions, we have investigated their properties when the cells are trapped and released. The efficacy of the transfusion treatment is also studied by comparing the relative changes in deformation and the relaxation-time of the cells in the two samples.

© 2012 Optical Society of America

**OCIS codes:** (000.2190) Experimental physics; (000.1430) Biology and medicine; (170.4520) Optical confinement and manipulation; (350.4855) Optical tweezers or optical manipulation.

## References and links

1. J. B. Herrick, "Peculiar elongated and sickle-shaped red blood corpuscles in a case of severe anemia," *Arch. Intern. Med.* **VI**(5), 517–521 (1910).
2. L. H. Pauling, H. A. Itano, S. J. Singer, and I. C. Wells, "Sickle cell anemia a molecular disease," *Science* **110**(2865), 543–548 (1949).
3. V. M. Ingram, "Gene mutations in human haemoglobin: the chemical difference between normal and sickle cell haemoglobin," *Nature* **180**(4581), 326–328 (1957).
4. C. Madigan and P. Malik, "Pathophysiology and therapy for haemoglobinopathies. Part I: sickle cell disease," *Expert Rev. Mol. Med.* **8**(09), 1–23 (2006).
5. M. P. Aguinaga, "Newborn screening and clinical management of children with sickle cell disease," in J. Navarro, ed., *Frontiers of Science in the 21st Century* (Cordillera, Lima, 2007), pp. 137–147.
6. S. Lanzkron, J. J. Strouse, R. Wilson, M. C. Beach, C. Haywood, H. Park, C. Witkop, E. B. Bass, and J. B. Segal, "Systematic review: Hydroxyurea for the treatment of adults with sickle cell disease," *Ann. Intern. Med.* **148**(12), 939–955 (2008).
7. E. Beutler, M. A. Lichtma, and B. S. Coller, "The sickle cell diseases and related disorders," in *Williams Hematology*, 6th ed. (McGraw-Hill, New York, 2001), pp. 581–606.
8. A. Kutlar, F. Kutlar, J. B. Wilson, M. G. Headlee, and T. H. J. Huisman, "Quantitation of hemoglobin components by high-performance cation-exchange liquid chromatography: its use in diagnosis and in the assessment of cellular distribution of hemoglobin variants," *Am. J. Hematol.* **17**(1), 39–53 (1984).
9. A. Ashkin, "Applications of laser radiation pressure," *Science* **210**(4474), 1081–1088 (1980).
10. A. Ashkin, J. M. Dziedzic, and T. Yamane, "Optical trapping and manipulation of single cells using infrared laser beams," *Nature* **330**(6150), 769–771 (1987).
11. F. Bordeleau, J. Bessard, N. Marceau, and Y. Sheng, "Measuring integrated cellular mechanical stress response at focal adhesions by optical tweezers," *J. Biomed. Opt.* **16**(9), 095005 (2011).
12. S. Rancourt-Grenier, M. T. Wei, J. J. Bai, A. Chiou, P. P. Bareil, P. L. Duval, and Y. Sheng, "Dynamic deformation of red blood cell in dual-trap optical tweezers," *Opt. Express* **18**(10), 10462–10472 (2010).
13. D. Erenso, A. Shulman, J. Curtis, and S. Elrod, "Formation of synthetic structures with micron size silica beads using optical tweezer," *J. Mod. Opt.* **54**(10), 1529–1536 (2007).
14. M. M. Brandão, A. Fontes, M. L. Barjas-Castro, L. C. Barbosa, F. F. Costa, C. L. Cesar, and S. T. Saad, "Optical tweezers for measuring red blood cell elasticity: application to the study of drug response in sickle cell disease," *Eur. J. Haematol.* **70**(4), 207–211 (2003).

15. M. M. Brandão, S. T. O. Saad, C. L. Cezar, A. Fontes, F. F. Costa, and M. L. Barjas-Castro, "Elastic properties of stored red blood cells from sickle trait donor units," *Vox Sang.* **85**(3), 213–215 (2003).
  16. G. B. Liao, P. B. Bareil, Y. Sheng, and A. Chiou, "One-dimensional jumping optical tweezers for optical stretching of bi-concave human red blood cells," *Opt. Express* **16**(3), 1996–2004 (2008).
  17. G. Athanassiou, A. Moutzouri, A. Kourakli, and N. Zoumbos, "Effect of hydroxyurea on the deformability of the red blood cell membrane in patients with sickle cell anemia," *Clin. Hemorheol. Microcirc.* **35**(1-2), 291–295 (2006).
  18. I. Dulińska, M. Targosz, W. Strojny, M. Lekka, P. Czuba, W. Balwierz, and M. Szymoński, "Stiffness of normal and pathological erythrocytes studied by means of atomic force microscopy," *J. Biochem. Biophys. Methods* **66**(1-3), 1–11 (2006).
  19. J. L. Maciaszek, B. Andemariam, and G. Lykotrafitis, "Microelasticity of red blood cells in sickle cell disease," *J. Strain Analysis Eng. Design* **46**(5), 368–379 (2011).
- 

## 1. Introduction

Since its discovery in the western world by James B. Herrick [1] in the year 1910, sickle cell anemia (SCA) has been identified as a genetic disease in which a point mutation in the  $\beta$ -globin gene located on chromosome 11 replaced one original nucleotide, adenine, with thymine. This single nucleotide substitution changes the codon from a CAG to a GTG resulting in the substitution of the amino acid valine for glutamic acid at the sixth position of the  $\beta$ -globin chain producing the sickle hemoglobin (HbS) [2,3]. This genetic mutation produces two distinct genotypes; heterozygotes (AS) resulting in sickle cell trait and homozygotes (SS) resulting in SCA.

In SCA, the normally round red blood cell (RBC), changes its shape and deformability under deoxygenating conditions, turning into banana-shaped cells known as sickle cells, which occlude the blood vessels in the microcirculation [4]. As a result patients with SCA suffer with acute, painful vasoocclusive crises. These symptoms do not appear until after six months of age when the  $\gamma$ -globin gene expression has primarily switched to  $\beta^S$ -globin gene expression resulting in the conversion from predominantly fetal hemoglobin (HbF) to sickle hemoglobin (HbS) instead of to normal adult hemoglobin (HbA). Although effective newborn screening programs in the country accurately identify babies affected with SCA at birth, the main purpose of this program is to place the SCA babies under proper health care management, which includes prophylactic penicillin until 5 years of age and age-appropriate vaccines [5]. In adults, the only FDA approved drug to treat sickle cell disease is hydroxyurea, which boosts the production of HbF [6]. The second commonly used treatment is regular intravenous transfusion of normal RBCs into the patient bloodstream [7]. The efficacy of either treatment is commonly measured by assessing the percentage of the different hemoglobin types in the patient's blood sample using HPLC [8]. The HPLC technique basically separates the negatively charged hemoglobin types by passing them through a positively charged cationic column. Flushing the chamber with different pH buffer solutions and measuring the different elution times for hemoglobin identification and relative percentages of the different hemoglobin types using a UV detector for hemoglobin quantitation.

Laser tweezers [9] are novel optical devices capable of conveniently trapping and manipulating living [10–12] or non-living [13] dielectric particles whose dimensions range from tens of nanometers to tens of microns [9]. In relation to SCA, laser tweezers have been used to study the properties of RBCs including measuring the therapeutic efficacy of the drug Hydroxyurea in SCA [14] and the integrity of stored RBCs drawn from patients with sickle cell trait [15]. Here we present a study that measures the efficacy of blood transfusion treatment in SCA patients by measuring the response of the RBCs to mechanical deformations using laser tweezers. We also present and correlate HPLC hemoglobin variant quantitation with laser tweezers individual cells measurements for RBCs from a transfused SCA patient and a healthy normal hemoglobin subject. We discuss experimental methods used for our measurements and the interpretation of the results obtained.

## 2. Experimental method

De-identified EDTA blood samples from a transfused SCA patient and two normal adult individuals were obtained from the Meharry Sickle Cell Center (MSCC), a major Hemoglobinopathy testing center located in Nashville, Tennessee. These samples were obtained from the individuals by either venipuncture or finger stick. Unless fresh, all samples used in the study were stored at 2°C at the MSCC. A biological material transfer agreement was processed between both institutions involved, MTSU and Meharry Medical College. The hemoglobin type quantitation was done by the Ultra2-HPLC from Trinity Bio-Tech (Kansas City, Kansas) at the MSCC. The SCA sample studied contained Hb S (53.68%), Hb A (39.72%), Hb A<sub>2</sub> (3.60%) and Hb F (3.0%). The patient had been transfused with packed RBCs from a normal adult hemoglobin blood donor. Hemoglobin types and relative percentages were also assessed by HPLC for each of the normal hemoglobin blood samples tested. The first blood sample (fresh) contained Hb A (97.1%), Hb A<sub>2</sub> (2.3%) and Hb F (0.6%) and the second (stored) contained Hb A (97.2%), Hb A<sub>2</sub> (2.8%) and Hb F (0%). Detailed information of the three blood samples is shown on Table 1.

In order to identify the RBCs in the transfused SCA patient blood sample, we used a simple size distribution measurement. First the three blood samples were diluted in fetal bovine serum in about a 1:100 ratio. Each of these samples was placed in a well slide, and several images were taken with a digital camera attached to the microscope and interfaced with a computer [see Fig. 3 below]. In each image several properties of the RBCs were measured using image processing, enhancement, and analysis software-Image-Pro Plus 6.2 (Media Cybernetics). This was carried out by programming Image-Pro Plus 6.2 to select bright

**Table 1. Relative Percentage of Hemoglobin types by HPLC and RBCs size measurements by Image-Pro**

Blood Sample	Healthy (Fresh 1)	Healthy (Stored)	Transfused SCA
Sex	M	M	M
Age	42	23	20
Draw date (Y/M/D)	2012/02/09	2012/01/31	2012/05/03
Delivery date (Y/M/D)	2012/02/09	2012/02/02	2012/05/07
HPLC measurement date (Y/M/D)	2012/02/13	2012/02/03	2012/05/07
HbA (%)	97.10	39.72	97.20
Relative % of each Hb type	02.30	03.60	02.80
HbA <sub>2</sub> (%)	00.00	53.68	00.00
HbS (%)	00.60	03.00	00.00
HbF (%)			
Size measurement date	2012/02/09	2012/02/09	2012/05/07
Average diameter ( $\mu\text{m}$ )	06.23	06.05	06.60
Standard deviation ( $\mu\text{m}$ )	00.56	00.60	00.90

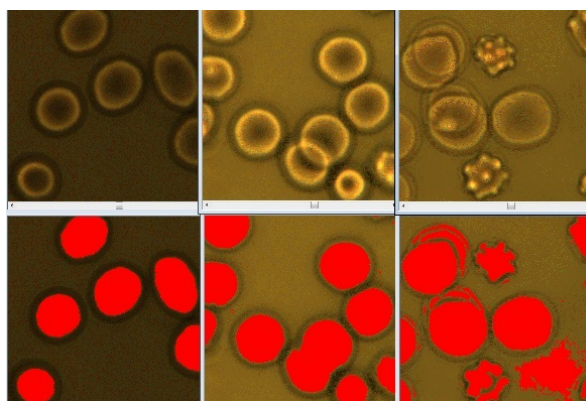


Fig. 1. Three blood samples diluted in fetal bovine serum [left to right: Normal Hb A (Fresh), Normal Hb A (stored), and transfused SCA patient. In the second row objects colored red represent the bright objects selected by Image-Pro for measurement.

objects in each images and take measurements for more than a dozen properties of these objects related to their sizes and shapes such as diameter, area, or perimeter in units of micrometers instead of pixels. Often, since the program takes the measurements for other bright objects in the image which are not RBCs, we needed to identify and delete these objects. A sample of the measurements for the three samples is shown in Fig. 1.

The size distributions for the blood samples from a transfused SCA patient, normal (fresh), and normal (stored) as measured by the mean diameter of the cells is shown by a histogram in Fig. 2. As one clearly sees from Fig. 2 the size of RBCs from the transfused SCA patient blood has a wider range ( $\sim 4\mu\text{m}$ - $9\mu\text{m}$ ) as compared to those from the normal hemoglobin blood samples ( $\sim 4.8\mu\text{m}$ - $7.2\mu\text{m}$ ) for fresh and ( $\sim 4.5\mu\text{m}$ - $7.5\mu\text{m}$ ) for stored. The average diameter of the RBCs from the transfused SCA patient blood is  $6.6 \pm 0.9\mu\text{m}$  whereas the RBCs from normal fresh is  $6.2 \pm 0.5\mu\text{m}$  and normal stored is  $6.05 \pm 0.6\mu\text{m}$ . The higher average size with a higher standard deviation is the result of the simultaneous presence of the abnormal sickle hemoglobin cells (which tend to be bigger in size) and the normal hemoglobin RBCs that came from the transfusion treatment with normal hemoglobin packed RBCs that the patient had received. The RBCs that come from the transfusion most probably would have average diameters in the overlapping region of the mean size distribution that we saw in the histogram shown in Fig. 2. By selecting the RBCs in the overlapping region we have studied the behavior of the cells in laser trap for both SCA transfused and the normal (fresh) blood samples.

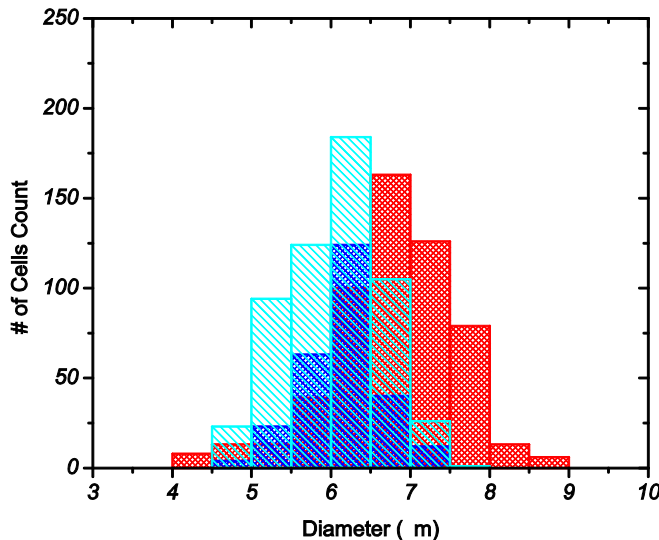


Fig. 2. The mean diameter of the RBCs distribution: SCA transfused blood sample (red), fresh (blue), and stored at  $2^\circ\text{C}$  (cyan). The last two are normal blood samples.

The basic element of the experimental set-up used to conduct this study is shown in Fig. 3. The laser source (LS) is a linearly polarized infrared diode laser (8 watts at 1064 nm) with a beam size of 4 mm. The power was controlled by a  $\lambda/2$ -wave plate (W) and polarizer (P) combination. To increase the beam size, we used a  $20\times$  beam expander (BE). However since this had expanded the beam too much, we inserted two pair of lenses (L1 and L2) with focal length of 20 cm and 5 cm, respectively. The beam expander and the two lenses together adjusted the beam to the appropriate size ( $\sim 2\text{ cm}$ ). The mirrors (M1-M4) were then used to align and direct the expanded beam through the laser port of an inverted microscope (IX 71-Olympus). A perfectly aligned expanded beam would then be redirected for a normal incidence angle at the center of the back of an objective lens (OL) using a dichroic mirror (DM) positioned at  $45^\circ$  inside the microscope. The OL has a  $100\times$  magnification and a 1.25 numerical aperture (Edmund Optics). The second pair of lenses (L3 and L4), which are

positioned at the appropriate distance from the back of the OL along with M4, are inserted in order to form the trap at the focal plane of the microscope. The microscope is equipped with piezo-driven (PS) stage to house and better manipulate the microscope slide and a digital camera (CCD) to take a live 2D bright-field contrast image of the sample in the slide using 30mW halogen lamp (HL). Both the piezo-driven stage and the digital camera are interfaced with a computer (PC).

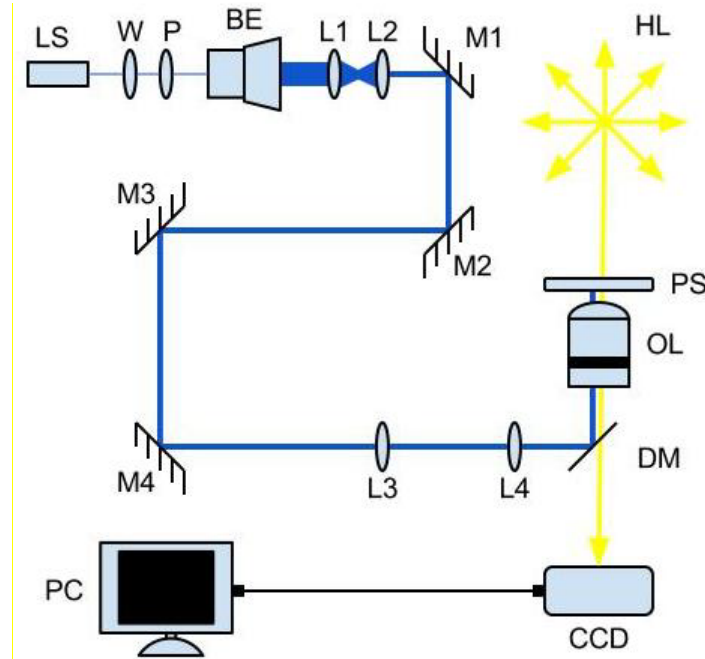


Fig. 3. The experimental set-up for single laser trap.

The behaviors we studied focused on the responses of the cells when they are confined by laser traps of varying strengths, kept inside the trap for fifteen seconds, released, and relaxed. To vary the strength of the trap the range of the power of the laser, which is measured near the middle of the two lenses, (L3 and L4) varied from about 30 mW to 280 mW. At the trap location, which is right outside the objective lens (OL) of the microscope, this power range corresponds to about 8 mW to 80 mW.

The measurement on fresh RBCs from the healthy individual was conducted first. For this purpose the blood sample was diluted with fetal bovine serum at 1:1000 dilutions. The diluted blood sample was placed on a well-slide and mounted on the piezo-driven stage (PS) of the microscope. Using the digital camera we took three consecutive images of the cell when free, lying on, or floating near to the bottom of the slide with its platelet side (its flat and wider side). We then opened the gate at the laser port of the microscope. The cell instantly flips and gets trapped with its platelet side parallel to the direction of the laser beam propagation. We immediately raised the trapped cell about twelve micrometers from where it was by raising the objective lens to avoid any effect caused by contact of the cell with the bottom of the slide. Three consecutive images were taken before the cell was released from the trap by closing the gate at the laser port. We then took images of the cell in fifteen seconds intervals for a couple of minutes after it was released from the trap. During this time as the cell relaxes it also keeps sinking slowly towards the bottom of the slide due to its weight. In order to keep it in focus, we have continuously adjusted the position of the objective lens. This procedure was repeatedly conducted for different trap strengths by changing the power of the laser. For better averages we have conducted a measurement for ten different cells at each power setting.

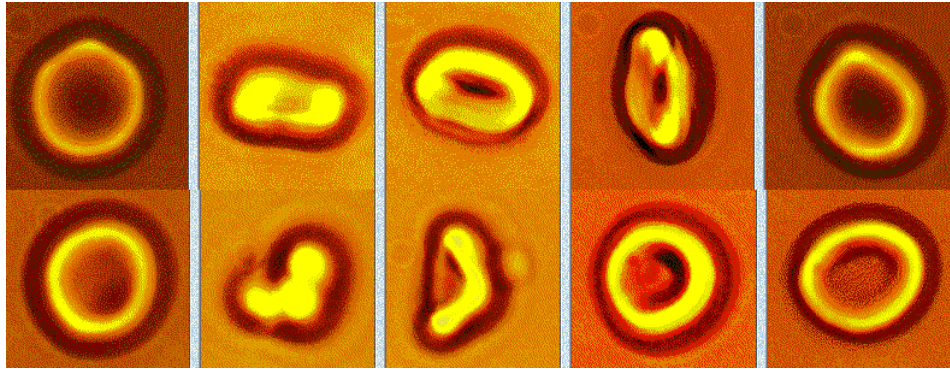


Fig. 4. Images of a cell (from the transfused SCA patient) trapped at 30mW (1st row) and at 230mW (2nd row) as it relaxes to its normal size and shape. These powers are measured at the laser port. From left to right it represents free cell, trapped cell, and sequence of released cell from the trap.

The exact same procedure is used for the RBCs from the transfused SCA patient blood sample. Sample images of this process for RBCs from a transfused SCA patient blood sample at two different powers are shown in Fig. 4.

### 3. Data analysis and results

We first conducted comparative analysis in relative size and shape changes due to direct laser trapping of RBCs from the healthy individual and RBCs from the transfused SCA patient. To conduct this analysis we used the maximum and minimum diameters of the RBC when it is free and trapped. The relaxation rates for the RBCs from the two samples are then studied by using the maximum diameters of the cells at different times starting from an initial time when the cell is released from the trap at different powers.

Image-Pro Plus 6.2 was used to measure the maximum and minimum diameters of each cell when it is free prior to trapping ( $d_0$ ) and inside the trap ( $d$ ) from the corresponding images. Using these two values we determined the relative change in the maximum and minimum diameters of the cell at a given power using  $\% \text{ change in diameter} = ((d_0-d)/d_0) \times 100\%$ . We then calculated the average values for the ten different cells at each power setting. The results are shown in Figs. 5a and 5b for maximum and minimum diameters, respectively. In both Figs. 5(a) and 5(b), blue represents the result for RBCs from a normal hemoglobin individual and red is for RBCs from a transfused SCA patient. Each of these data points represents the average value of ten cell measurements at the specified power. The bars represent the standard deviation in values of those measurements. These results show that both normal and transfused RBCs have reduced size inside the trap in either case. This is mainly because of two reasons. The first one is that the cell begins to contract towards the center of the trap as the power of the laser trap becomes stronger due to an increase in intensity gradients. This contraction misleadingly seems to be significantly higher in the change in the minimum diameter. However, this significantly higher change is mainly due to the fact that the cells flipped inside the trap and the image that the camera took is the side view which has a much narrower transverse diameter (the minimum diameter) than longitudinal diameter. Therefore, the change is significantly higher for the minimum diameter as compared to the free cell (which is nearly circular) minimum diameter which is about the same as the maximum diameter. As it contracts it also begins to flip back to its original state and also slightly expand along its narrow transverse dimension which eventually results in a sort of spheroid shape at higher power. This is the main reason that the change for the minimum diameter reduces at higher power as can be seen in Fig. 4(b). Comparison of the normal and the transfused results show that the relative change is higher in the normal for both the maximum and minimum diameters especially at a relatively low power. However,

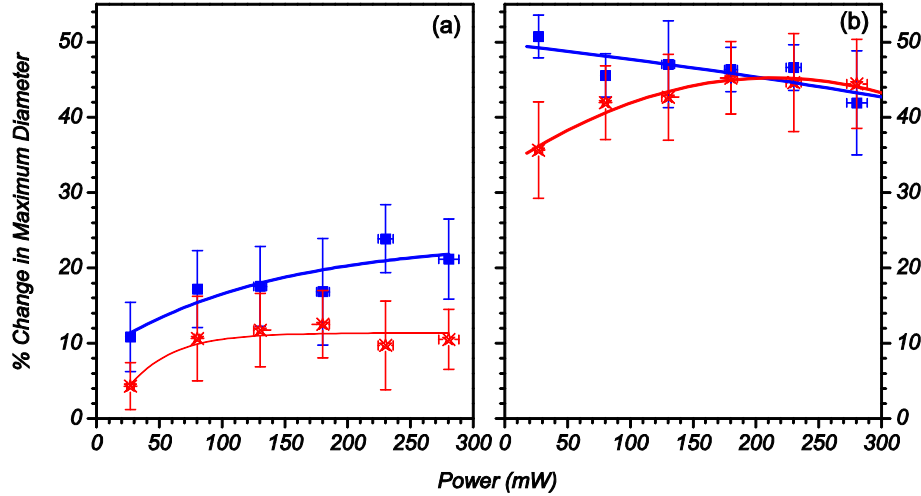


Fig. 5. The percentage change in the maximum (a) and minimum (b) diameters of the cell inside the trap relative to the diameter of the cell when it is free as function of the laser power. Healthy (blue) and transfused SCA (red).

this behavior essentially becomes the same at higher powers for the minimum diameter for both the normal and the transfused RBCs.

The response of the cells in the two samples displayed in Fig. 5 depends on the strength of the trapping force acting on the cells. This force is proportional to the power trapping the cell, which depends on the beam size of the laser beam in the trapped cells. Following a similar model discussed by Lian et al. [16] we have effect of the beam size using Ray-optics. The beam size ( $w$ ) depends on the angle of incidence of a ray on the trapped cell ( $\theta$ ), the angular position with respect to the beam axis [ $-\alpha_{max} \leq \alpha \leq \alpha_{max}$ ], the size of the cell, and the trap position. The maximum angular position of the incident ray with respect to the beam axis ( $\alpha_{max}$ ) is determined by the numerical aperture (NA) of the objective lens, the refractive index of the surrounding medium ( $n_1$ ), and is given by  $NA = n_1 \sin(\alpha_{max})$ . For our trap  $NA = 1.25$  and  $n_1 = 1.28$  which gives  $\alpha_{max} = 78^\circ$ . If the beam focused by the OL directed along the negative z-axis traps a RBC with a diameter  $d_0$ , then the cell would flip inside the trap with its larger circumference on the x-y plane. If the center of gravity of the cell is chosen to be the origin, then position of the trap would be  $z_0$  on the positive z axis. For this trap, following the method by Lian et al. [16], the beam size can be expressed as  $w = (d_0 \cos(\alpha + \theta) - z_0) \tan(\alpha_{max})$ . Therefore, for a Gaussian beam the power ( $P$ ) trapping the cell, which decays exponentially ( $\sim \exp(-r^2/w^2)$ ) as the distance from the beam axis ( $r$ ) increases, depends on the beam size inside the trap which varies with the size of the cell ( $d_0$ ) and position of the trap ( $z_0$ ). The RBCs from the transfused blood sample have a bigger size than the RBCs from the normal sample. This may seem the beam size becomes bigger and the power gets weaker for the RBCs from the transfused blood sample. But the bigger cells tend to be heavier causing the center of gravity of the cell to shift down which increase  $z_0$ . This most likely counter balance the beam size increase caused by the size of the cell and may not have significant effect in the result.

We have studied the relaxation rates of the RBCs using the maximum diameter of the cells from the initial time when the cells are inside the trap and immediately after they are released with 15 second intervals for a duration of about 75 seconds. Following a similar procedure described above, the relative change in the maximum diameter of the cell released from the trap at a given power was calculated using  $\% \text{ change in diameter} = ((d_0 - d)/d_0) \times 100\%$ , where  $d_0$  is the same corresponding average maximum diameter of the free cells we used earlier while  $d$  is the average maximum diameter of the cell released from the trap at different times. We then plotted this percent difference as a function of time for the different powers of the

trap. The results for the RBCs from the normal HbA individual and transfused SCA patient blood samples are shown in Figs. 6(a) and 6(b), respectively. In both graphs, the data point plotted starts  $t = 15$  s where the first image was captured after the power of the laser cut off at  $t = 0$ . The relative changes in maximum diameters for the RBCs in both samples at different powers are color coded in the same way: 30 mW (red), 80 mW (green), 130 mW (yellow), 180 mW (blue), 230 mW (cyan) and 280 mW (magenta). When the cells are fully relaxed, they recover the exact same size and shape of the free cell at a given time. The measured average maximum diameter of the relaxed cells is expected to be the same as the average maximum diameter of the corresponding free cells (i.e.  $d = d_0$ ). Therefore, the relative change approaches to a zero value as the cell fully relaxes and recovers its original size and shape in contrary to when it is not in which the relative change has a maximum value.

We clearly see from Figs. 6(a) and (b), at the initial time after the cell released from the trap ( $t = 15$  s), the results for the RBCs from the healthy blood sample show significant differences at different powers than those from the transfused SCA patient. This is mainly because the RBCs in the healthy blood sample nearly all ( $> 97\%$ ) have the normal hemoglobin (HbA) type; it is expected for these to be more elastic and significantly reduced in size due to the intensity gradient laser trap when the cells were inside the trap at  $t = 0$  (Fig. 5(a)).

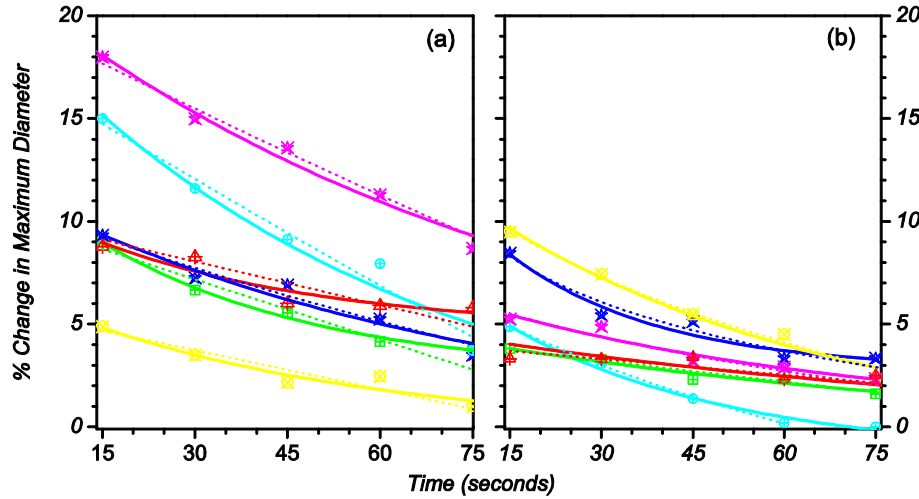


Fig. 6. The percent difference of the average maximum diameter of the cells released from the trap relative to the corresponding free cells as a function of time at 30mW (red), 80mW (green), 130mW (yellow), 180mW (blue), 230mW(cyan) and 280mW (magenta): (a) For RBCs (fresh) from a normal Hb A and (b) RBCs from a transfused SCA patient.

On the other hand the relative HbA % in the transfused SCA blood sample is  $< 40\%$  compared to the relative sickle hemoglobin (HbS) % which is 53.68% of the total Hb content (Table 1). RBCs with HbS are less elastic and do not reduce in size significantly by the intensity gradient laser trap at  $t = 0$  (Fig. 5(b)). The increased stiffness of RBCs with abnormal HbS agrees with previous studies based on micropipette and filtration [17], and atomic force microscopy techniques [18,19]. Therefore, for normal HbA RBCs, the relative change in the average maximum diameter of the relaxed cells with respect to the corresponding free cells is still going to be higher at the initial time ( $t = 15$  s) after release from the trap (Fig. 6(a)) compared to those from the transfused SCA patient (Fig. 6(b)). Even for such small relative deformation, the curves fitted to the data points at different powers in Fig. 6(a) and (b) indicate that the RBCs from the transfused SCA blood sample appear to relax at a relatively slower rate than those from a normal HbA blood sample. This can be observed, at least for low power, from the relatively smaller slopes of the curves in Fig. 6(b) than those in Fig. 5(a).

In order to verify these behaviors, we have defined and calculated a time constant for the relaxation rates as function of the laser power for the cells in the two blood samples. The time

constant is calculated using two functions that best fitted the data points for the relative change of the maximum diameter shown in Fig. 6. These functions are determined using graph programming software Origin 7.5. One of these functions is an exponential decaying function [ $f_1(t) = A_0 + A_1 \exp\{-(15 - t)/t_0\}$ ] which is shown by the solid lines. The other is a logarithmic function [ $f_2(t) = B_0 - B_1 \ln(t - B_2)$ ] which is shown by the dotted line in Fig. 6. The constants  $A_0$ ,  $A_1$ ,  $t_0$ ,  $B_0$ ,  $B_1$ , and  $B_2$  have different values at different powers. The time constant ( $\tau$ ) is defined as the time for which the relative change in maximum diameter immediately after the cell is released from the trap (as predicted by the two functions  $f_{1,2}(t = 0)$ ) is reduced by half. We then determined two time constants by solving the two functions for each power. The average of the two as a function of the trap power is plotted in Fig. 7. The data points and the fitting curve shown in red are for the RBCs from the transfused SCA blood sample and those shown in blue are for RBCs from the normal HbA blood sample.

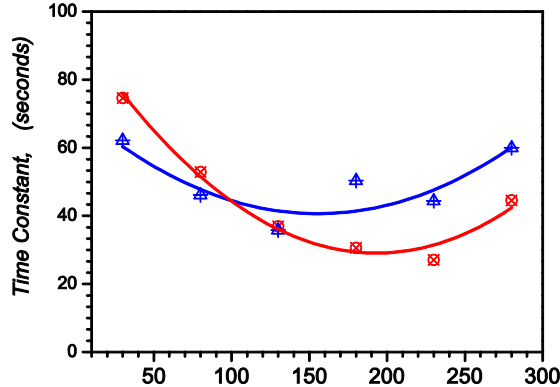


Fig. 7. The relaxation time constant of the cells after it is released from the trap as function of power. Normal Hb A individual (blue) and transfused SCA patient (red).

The data in Fig. 7 shows that the time constant predicts interesting behaviors for the relaxation rate of the RBCs after release from the trap as the power of the trap changes. For the RBCs from both samples, the time constant first begins to decrease as the power increases before it reaches a minimum value and then begins to increase as the power becomes higher. This indicates that for both samples, the RBCs relax relatively faster as the power of the trap increases up to certain limited power. However, when the power increases further and exceeds these limits, the time constant appears to increase and the cell seems to relax more slowly. From both of the parabolic curves in Fig. 7 we may predict that the time constant reaches a minimum value of  $\sim 40$  s at about 160 mW for the RBCs from the normal HbA blood sample and minimum value of  $\sim 29$  s at about 190 mW for the RBCs from the transfused SCA blood sample. A reasonable explanation for the fast relaxation rates (decrease in the time constant) up to this limit in both cases could be the inevitable heating effect resulting from increasing the power of the trapping laser. At relatively high power the infrared (1064nm) laser energy can be more strongly absorbed by the water molecules, elevating thermal vibrations in the RBCs which could lead to fast recovery of its original size through expansion. However, this heating could have an effect in compromising the integrity of the cellular cytoskeleton which plays a major role in the visco-elastic properties of RBCs. This effect appears to be greater in the normal than the transfused blood samples. At some extreme powers, we have observed the cell membranes rupture, become charged, and are ejected from the trap. At extremely low power, the results in Fig. 7 predict a higher time constant for the RBCs from the transfused blood sample as expected.

#### 4. Conclusion

We determined the relative percentage of the different hemoglobin types in blood samples from two normal HbA individuals and in one SCA patient treated with packed-RBCs

transfusion. We also conducted a simple size distribution measurement in those samples to identify the RBCs coming from the blood transfusion. In addition, we have studied how those transfused RBCs in the overlapping region of the size distribution in the transfused SCA patient respond to direct laser trapping in comparison to RBCs from a normal HbA individual. The results show that the relative size change is higher for the RBCs in a normal individual than those in a transfused SCA patient. This is mainly because of the presence of more sickle hemoglobin than the normal hemoglobin in the blood sample. We have also studied how the cells from the two samples relax and recover their size and shape after they are released from a trap with different strengths by analyzing the relaxation rates of the cells. The relaxation rates for the RBCs from the healthy blood sample are relatively faster than those from the transfused SCA blood sample at a relatively low power. For both the healthy and transfused SCA, interestingly, the RBCs show that the cells released from a high power trap relax relatively faster than those released from a low power trap up to a certain limit. This is probably due to an increase in the fraction of the energy absorbed by the water molecules in RBCs in the infrared region at high intensity which could facilitate the relaxation of the cells through thermal vibration. Changes in deformability and relaxation-time of the RBCs by the techniques described in this study could be correlated to the efficacy of transfusion treatments in SCA.

### Acknowledgments

Funding/Support: Partial funding for this activity came from MTSU's URECA, NSF FirstStep Grant, and the Department of Health and Human Services/Office of Minority Health (MPCMP081013 B OMH-MMC-1-09). The views expressed in written materials or publications and by speakers and spokespersons do not necessarily reflect the official policies of the Office on Minority Health and Health Disparities, nor does mention by trade names, commercial practices, or organizations imply endorsement by the U.S. government.